New Solar Physics with Solar-B Mission
ASP Conference Series, Vol. 369, 2007
K. Shibata, S. Nagata, and T. Sakurai

Plans to Observe Flare-Associated Waves with *Solar-B*

Noriyuki Narukage

Kwasan and Hida Observatories, Kyoto University, Yamashina, Kyoto 607-8471, Japan

Abstract. The *Solar-B* will carry Solar Optical Telescope (SOT), X-Ray Telescope (XRT), and EUV Imaging Spectrometer (EIS) on board and will be launched in 2006. We expect SOT, XRT, and EIS will detect the origin of Moreton waves, coronal X-ray waves, and line-of-sight velocity of waves, respectively. In preparation for *Solar-B*, we examine the detectable possibility of waves with these telescopes and suggest methods for observation.

1. Introduction

When solar flares occur, flare-associated waves are sometimes observed in some wavelengths (see Figure 1). Moreton waves are flare-associated waves observed to propagate across the solar disk in Hα (Moreton 1960; Smith, Harvey 1971). The front usually becomes visible only at a distance of more than 100,000 km from the place of its origin. Some flare-associated waves can be followed on the disk up to distance exceeding 500,000 km and they propagate with fairly constant speed. Figure 2 shows the observable region of the flare-associated waves. They propagate at speeds of 500–1500 km s^{-1} with arc-like fronts in somewhat restricted angles. The Moreton wave has been identified as the intersection of a coronal MHD fast-mode weak shock and the chromosphere (Uchida 1968, 1974). The downward motion of the chromospheric plasma caused by the shock wave is observed in Hα as the Moreton wave front. However, the generation mechanism of a Moreton wave has not been made clear yet.

Recently, the Soft X-ray Telescope (SXT) on board *Yohkoh* discovered "X-ray waves" associated with flares (Khan & Hudson 2000; Hudson et al. 2003) (see Figure 1). Some simultaneous observations of Moreton waves and X-ray waves were also reported (Khan, Aurass 2002; Narukage et al. 2002, 2004). Narukage et al. (2002, 2004) examined the jump condition across the X-ray wave and identified the X-ray wave as an MHD fast-mode shock, i.e. the coronal counterpart of the Moreton wave. The study of the X-ray wave has just begun.

The *Solar-B* will carry Solar Optical Telescope (SOT), X-Ray Telescope (XRT), and EUV Imaging Spectrometer (EIS) on board and will be launched in 2006. The purpose of this paper is to examine the detectable possibility of the flare-associated waves (i.e., the chromospheric Moreton waves and the coronal X-ray waves) with *Solar-B* and to suggest the observational methods and targets in preparation for *Solar-B*. We expect SOT, XRT, and EIS will detect the origin of Moreton waves, coronal X-ray waves, and line-of-sight velocity of these waves, respectively.

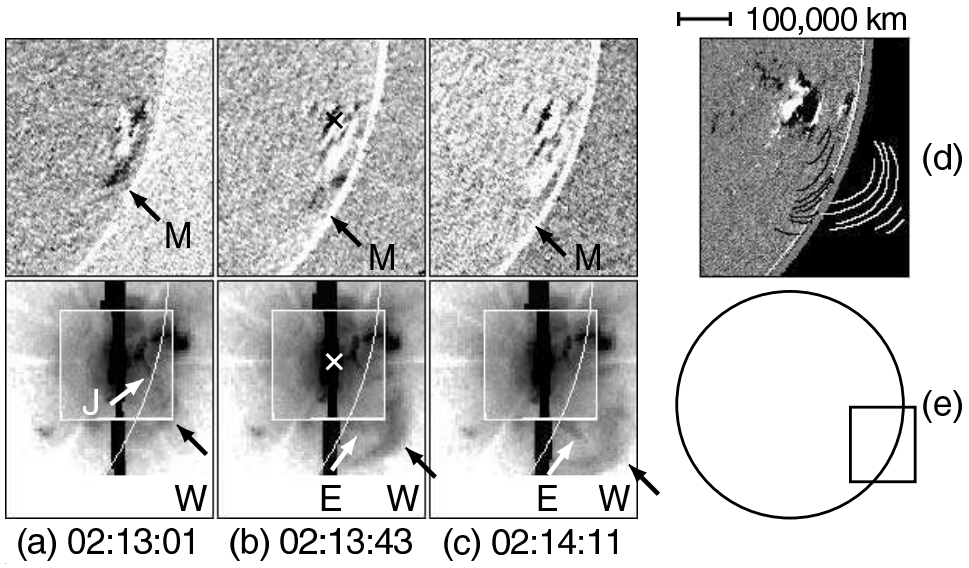

Figure 1. Observed images on 2000 March 3, at NOAA AR 8882. Top panels of images (a)–(c) are Hα +0.8 Å "running difference" images of a Moreton wave (black arrows "M"). Bottom panels of images (a)–(c) are negative soft X-ray images of an X-ray wave (black arrows "W"), ejecta (white arrows "E") and a jet (white arrow "J") taken with the Al-Mg filter. The crosses in image (b) are the flare site. We assume that the brightest region in Hα is the flare site. Image (d) shows the wave fronts of the Moreton wave from 02:12:01 to 02:15:01 UT (black lines) and the X-ray wave from 02:13:01 to 02:14:11 UT (white lines) overlaid on the photospheric magnetic field observed at 01:35:02 UT. These wave fronts were determined visually. The box and circle shown in image (e) are the field of view of images (a)–(c) and the limb of the Sun, respectively.

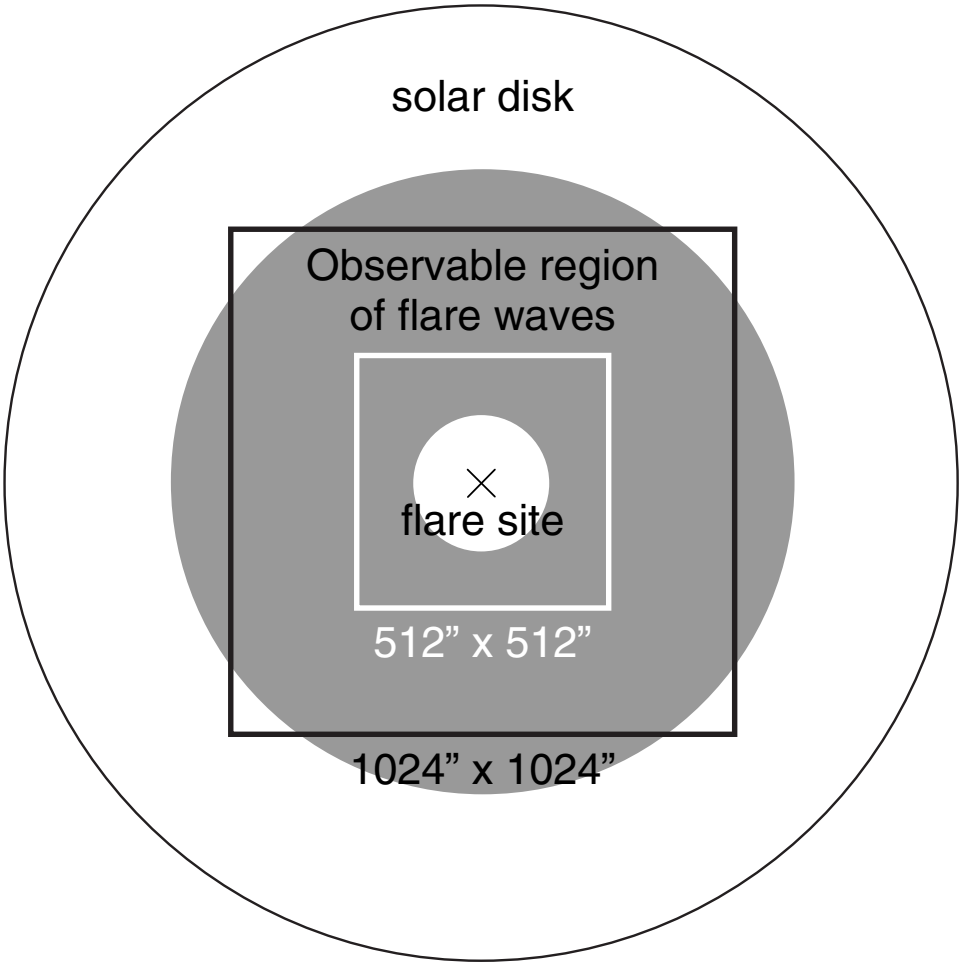

Figure 2. Observable region of the flare wave (gray area) when a flare occurs at the center of the solar disk (black cross). The white and black boxes show the regions of 512" × 512" and 1024" × 1024", respectively.

2. Solar Optical Telescope and EUV Imaging Spectrometer

Solar Optical Telescope (SOT) can observe the chromospheric Moreton wave in Hα. However, the field of view (164" × 328") is not enough to observe the propagation of the Moreton wave (see Figure 2). Meanwhile, the spatial resolution and time resolution are very high. We expect the SOT to detect the origin of the Moreton waves. The simultaneous observation in Hα with SOT and ground telescopes, which observe full-disk images at a high time resolution (e.g., Flare Monitoring Telescope (FMT) and Solar Magnetic Activity Research Telescope (SMART) at Hida Observatory of Kyoto University), is important for the study of Moreton waves. Meanwhile, SOT can measure vector magnetic field. We consider that the filament eruptions and magnetic field in flare region are keys to the basic question of how the shock wave is generated. Hence, SOT is the useful instrument to examine this question.

The EUV Imaging Spectrometer (EIS) can measure the line-of-sight velocity. We estimate the coronal plasma velocity just behind the Moreton wave (fast-mode MHD shock) to be about 100–200 km s^{-1} (Narukage et al. 2002), which would be observed at 50–100 km s^{-1} along the line-of-sight with EIS. This observation is important for the evidence of Uchida's model (Uchida 1968).

3. X-Ray Telescope

3.1. X-Ray Wave

X-Ray Telescope (XRT) is the successor to *Yohkoh*/SXT and observes the solar corona in soft X-rays. We expect XRT to detect the X-ray waves more frequently and clearly than SXT. In this section, we examine the detectable possibility of the X-ray wave based on the results of Narukage et al. (2002).

At first, we discuss the selection of the field-of-view, pixel size and time cadence based on the statistical analysis of the Moreton waves. The flare waves can propagate to distances exceeding 500,000 km. The field of view is required larger than 512" × 512" to observe the propagation of the X-ray wave (see Figure 2). The pixel size should be smaller than 4" × 4", because the thickness of the waves are about 40,000 km. When the flare wave propagates to 500,000 km at the typical speeds, i.e., 500–1500 km s^{-1}, we can observe it for less than 270–800 seconds. For the estimation of the temperature and volume emission measure, we need the images observed with at least 2 kinds of filters. Hence, the observation needs as high a cadence as possible. The combinations of the field-of-view, pixel size and time cadence determine the data size and are limited by the data recorder capacity. The data recorder is shared by three telescopes. The quota of XRT data is 15% of toatl capacity (= 1.2Gbits = 150Mb).

Table 1. Design of X-ray analysis filters (Kano, R. et al. 2004).

Name	Metal	Substrate
Thin-Al/Mesh	Al 1600 Å	Mesh
Thin-Al/Poly	Al 1250 Å	Polyimide 2500 Å
C/Poly	C 4800 Å	Polyimide 2500 Å
Ti/Poly	Ti 2300 Å	Polyimide 2500 Å
Thin-Be	Be 9 μm	Mesh
Med-Be	Be 30 μm	–
Med-Al	Al 12.5 μm	–
Thick-Al	Al 25 μm	–
Thick-Be	Be 1 mm	–

The XRT has 9 filters to detect the plasma in the temperature range ∼ 1M–10M K (Table 1 and Figure 3). The selection of these filters is important to observe the X-ray waves. Based on the X-ray wave observed with *Yohkoh*/SXT on 1997 November 3 (Narukage et al. 2002), the density jumped from $1.00 \times 10^{8.5}$ to $1.31 \times 10^{8.5}$ across the shock front and temperature from 2.25 MK to 2.78 MK. Using this quantities, we calculate the XRT intensities ahead of (I_{X1}) and behind (I_{X2}) the X-ray wave front, and their ratios (I_{X2}/I_{X1}) in Table 2. To

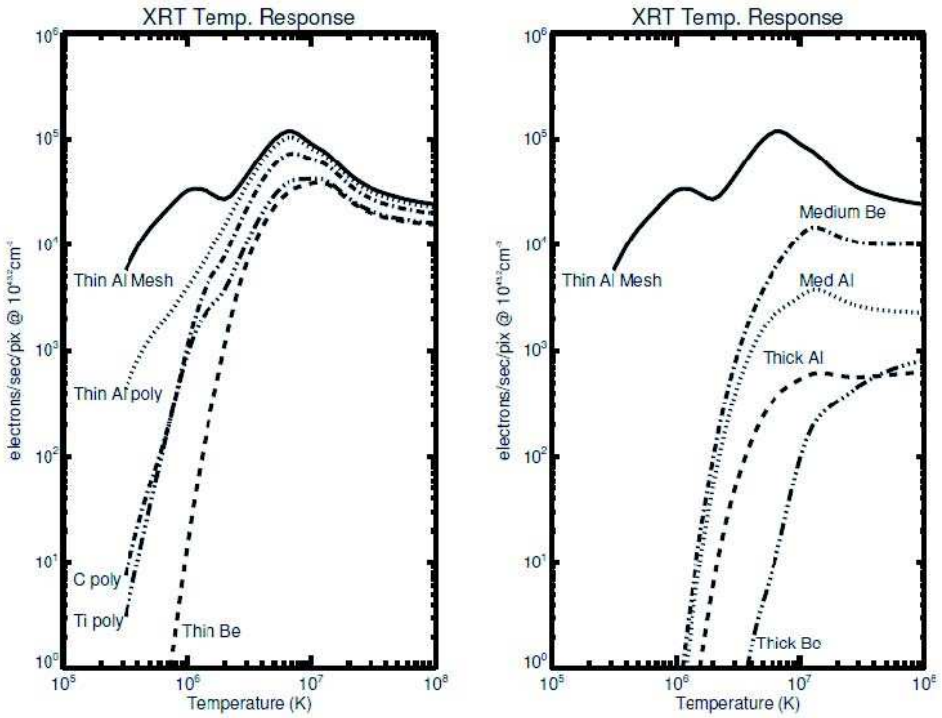

Figure 3. Temperature response functions of XRT filters. (Figure 3 in Kano, R. et al. (2004))

Table 2. Estimated intensities of the X-ray wave observed with XRT filters.

filter	I_{X1} [DN sec^{-1} arcsec^{-2}]	I_{X2} [DN sec^{-1} arcsec^{-2}]	I_{X2}/I_{X1}
Entrance	280	578	2.06
Thin Al Mesh	191	444	2.33
Thin Al Poly	120	347	2.68
C Poly	71	205	2.91
Ti Poly	36	101	2.83
Thin Be	14	58	4.16
Medium Be	1	6	4.61
Medium Al	1	3	4.50
Thick Al	0	0	–
Thick Be	0	0	–

recognize the shock against the background, it is desirable that the intensity (I_{X2}) and intensity ratio (I_{X2}/I_{X1}) are large. To estimate the temperature and emission measure, we need 2 filters and it is desirable that their temperature response functions are not similar. Considering above conditions, we concluded that the C-poly and Thin-Be filters are suitable to detect the *Solar-B*.

Next, we examine the enough exposure time (t [sec]) to suppress the effect of photon noise:

$$\sigma(t)[\mathrm{DN}] = N^{1/2}[\mathrm{photon}] \times C[\mathrm{e}^-/\mathrm{photon}]/57[\mathrm{e}^-/\mathrm{DN}], \quad (1)$$

where N and C are number of photons and conversion factor (= 300 [e$^-$ / photon]), respectively. We note that the photon noise is superior to the other noise, e.g., system noise (< 30e$^-$) and dark (= 0.1e$^-$/sec/pix). To suppress the effect of photon noise, the exposure time should satisfy the following condition:

$$(I_{X2} - I_{X1})t > 3\sigma(t). \quad (2)$$

The estimated minimum exposure times are shown in Table 3.

Table 3. Minimum exposure time to suppress the effect of photon noise.

	pixel size		
filter	1" × 1"	2" × 2"	4" × 4"
C poly	378	95	24
Thin Be	418	105	26

Table 4. X-ray wave observing mode.

	selection	note
filter	C poly & Thick Be	
pixel size	2" × 2"	FOV : 768" × 768"
image size	384 pix × 384 pix	Data size : 1728 kbits / image
compression	loss less	Compressed size : 864 kbits / image (50% compression)
exposure time	> 125 ms	< saturation (see Kano, R. et al. (2004) Table 4.)
time cadence	15 sec	30 sec / 1 filter set
obs. time	900 sec	60 images (30 sets) = 50.6 Mbits

Based on the above examinations, we suppose the "X-ray wave observing mode". Table 4 shows the minimum-data-size plan. XRT is the most suitable telescope for the X-ray wave (coronal shock wave). When the filter selection for the flare-mode is discussed, the detectability of the X-ray wave should be considered.

3.2. Counterpart of EIT Wave

Recently many large-scale coronal transients have been discovered with Extreme ultraviolet Imaging Telescope (EIT) on board *Solar and Heliospheric Observatory (SOHO)*. These features are now commonly called "EIT wave" (Moses

et al. 1997; Thompson et al. 1998). The observations of EIT waves covered a wavelength range centered on 195 Å, dominated by a Fe XII line emitted near 1.5×10^6 K at typical coronal density. The *Solar-B*/XRT has the Thin Al Mesh filter which can observe the coronal plasma at a temperature of $\approx$ 1 MK (see Figure 3). This filter is expected to detect the counterpart of EIT waves.

Moreover, Warmuth et al. (2005) presented the first observations of global coronal waves obtained with the Solar X-Ray Imager (SXI) aboard the *GOES-12* satellite. These "SXI waves" were observed in the OPEN configuration without any filter, which is sensitive to temperatures of $\approx$ 3 MK. The configurations of SXI waves are similar to EIT waves. This means that a coronal transient that is observable with EIT will generally also be imaged by SXI. Hence, there is a large possibility that the XRT also detect the counterpart of EIT waves.

4. Summary and Discussion

In this section, we discuss the scientific target of the flare-associated wave.

How much flare-released energy does spend on the shock generation and propagation? This is a very basic and important question. To solve this question, observations of shock waves with XRT are indispensable, because the soft X-ray data give us the physical quantities.

In the event observed on 2000 March 3, the fast-mode Mach number, which was estimated with the intensity of the X-ray wave, decreased at a constant ratio. The timing when the Mach number becomes "1" corresponds to the disappearance of the Moreton wave (Narukage et al. 2004). This result is clear evidence for the Uchida model. Analyzing the X-ray waves observed with XRT, we will be able to estimate the physical quantities of the shock waves during the propagation. Especially, the change of the quantities is important.

In all of the Moreton wave events observed at the Hida observatory, Hα filaments erupted in the same direction after the waves propagated. Before the eruption, the filaments were invisible in Hα. In some cases of X-ray waves, X-ray ejecta were also observed (Narukage et al. 2004) (see Figure 1). We consider this point as the clue to elucidate the generation mechanism of the flare-associated wave. We expect SOT and XRT to detect the origin of the flare-associated waves. Meanwhile, vector magnetic field in flare region measured with SOT is also key to examine the generation mechanism.

Table 5. Estimated numbers of the flare-associated waves from 2006 to 2009.

Year	2006	2007	2008	2009
X-ray wave	1	1	2	11

We note that it is difficult to identify the X-ray waves based on only X-ray images, because X-ray waves are faint (especially, in *Yohkoh*/SXT images) and confused with other phenomena, e.g., expanding loop or ejection. Hence, the simultaneous observations in multi-wavelength are important, e.g., in Hα where Moreton waves are observed and radio wave where type-II radio bursts are detected, etc.

Finally we mention the frequency of the flare-associated waves after *Solar-B* is launched. Based on the observations of the Moreton waves at the Hida Observatory, the flare-associated waves would occur associated with 10% of X or M-class flares. If the flare frequency is the same as 11 years before, until 2009 there would be only a few waves per year. Table 3 shows the estimated numbers of the flare-associated waves from 2006 to 2009. Although these numbers are underestimates, there is only a small number of opportunities to observe the flare-associated waves. Hence the observational plan should be made carefully and effectively.

References

Hudson, H. S., Khan, J. I., Lemen, J. R., Nitta, N. V., & Uchida, Y. 2003, Sol. Phys., 212, 121
Kano, R. et al. 2004, ASP Conference Series, 325, 15
Khan, J. I., & Aurass, H. 2002, A&A, 383, 1018
Khan, J. I. & Hudson, H. S. 2000, Geophys. Res. Letters, 27, 1083
Moreton, G. E. 1960, AJ, 65, 494
Moses, D., et al. 1997, Solar Phys. 175, 571
Narukage, N., Hudson, H. S., Morimoto, T., Akiyama, S., Kitai, R., Kurokawa, H., and Shibata, K. 2002, ApJ, 572, L109
Narukage, N., Morimoto, T., Kadota, M., Kitai, R., Kurokawa, H., and Shibata, K. 2004, PASJ, 56, L5
Smith, S. F., & Harvey, K. L. 1971, in Physics of the Solar Corona, ed. C. J. Macris (Dordrecht: Reidel), 156
Thompson, B. J., Plunkett, S. P., Gurman, J. B., et al. 1998, Geophys. Res. Letters, 25, 246
Uchida, Y. 1968, Sol. Phys., 4, 30
Uchida, Y. 1974, Sol. Phys., 39, 431
Warmuth, A., Mann, G., and Aurass, H. 2005, ApJ, 626, L121